
This is an electronic reprint of the original article.
This reprint may differ from the original in pagination and typographic detail.

Bouravleuv, Alexei; Cirilin, George; Sapega, Victor; Werner, Peter; Savin, Alexander;
Lipsanen, Harri

Ferromagnetic (Ga,Mn)As nanowires grown by Mn-assisted molecular beam epitaxy

Published in:
Journal of Applied Physics

DOI:
[10.1063/1.4799624](https://doi.org/10.1063/1.4799624)

Published: 01/01/2013

Document Version
Publisher's PDF, also known as Version of record

Please cite the original version:
Bouravleuv, A., Cirilin, G., Sapega, V., Werner, P., Savin, A., & Lipsanen, H. (2013). Ferromagnetic (Ga,Mn)As nanowires grown by Mn-assisted molecular beam epitaxy. *Journal of Applied Physics*, 113(14), 1-6. Article 144303. <https://doi.org/10.1063/1.4799624>

This material is protected by copyright and other intellectual property rights, and duplication or sale of all or part of any of the repository collections is not permitted, except that material may be duplicated by you for your research use or educational purposes in electronic or print form. You must obtain permission for any other use. Electronic or print copies may not be offered, whether for sale or otherwise to anyone who is not an authorised user.

Ferromagnetic (Ga,Mn)As nanowires grown by Mn-assisted molecular beam epitaxy

Alexei Bouravleuv, George Cirlin, Victor Sapega, Peter Werner, Alexander Savin, and Harri Lipsanen

Citation: *Journal of Applied Physics* **113**, 144303 (2013); doi: 10.1063/1.4799624

View online: <http://dx.doi.org/10.1063/1.4799624>

View Table of Contents: <http://aip.scitation.org/toc/jap/113/14>

Published by the [American Institute of Physics](#)

AIP | Journal of
Applied Physics

Save your money for your research.
It's now **FREE** to publish with us -
no page, color or publication charges apply.

Publish your research in the
Journal of Applied Physics
to claim your place in applied
physics history.

Ferromagnetic (Ga,Mn)As nanowires grown by Mn-assisted molecular beam epitaxy

Alexei Bouravleuv,^{1,2,3,a)} George Cirlin,^{1,2,4} Victor Sapega,¹ Peter Werner,⁵ Alexander Savin,³ and Harri Lipsanen³

¹Ioffe Physical Technical Institute RAS, 194021 St. Petersburg, Russia

²Laboratory of Epitaxial Nanotechnologies, St. Petersburg Academic University RAS, 194021 St. Petersburg, Russia

³School of Electrical Engineering, Aalto University, FI-02150 Espoo, Finland

⁴Institute for Analytical Instrumentation RAS, 190103 St. Petersburg, Russia

⁵Max Planck Institute of Microstructures Physics, D-06120 Halle, Germany

(Received 16 January 2013; accepted 21 March 2013; published online 8 April 2013)

(Ga,Mn)As nanowires were grown by molecular beam epitaxy using Mn as a growth catalyst on GaAs(001) substrates at 485 °C, i.e., at intermediate temperatures higher than ones used for the growth of (Ga,Mn)As thin films, but lower than the ordinary temperatures of Au-assisted growth of GaAs nanowires. (Ga,Mn)As nanowires obtained with typical lengths between 0.8 and 4 μm and diameters 50–90 nm do not have defects, such as dislocations or precipitates, except for the stacking faults lying parallel to the growth direction. The investigation of magnetic and optical properties has been carried out not only for as-grown samples with nanowires but also for peeled off nanowires from the host substrate. The results obtained demonstrate that (Ga,Mn)As nanowires exhibit ferromagnetic ordering around 70 K. © 2013 American Institute of Physics. [<http://dx.doi.org/10.1063/1.4799624>]

I. INTRODUCTION

The ferromagnetic properties of Mn-doped III-V semiconductors have attracted intensive attention over the last decades¹ since the combination of semiconductor and ferromagnets properties makes it possible to achieve radically new functionality in electronic or so-called spintronic devices. Among such diluted magnetic semiconductors (DMS), the most extensively studied material is (Ga,Mn)As.^{2,3} It can be obtained by different epitaxial growth methods, e.g., by molecular beam epitaxy (MBE). If a Mn atom substitutes a Ga cation site, it can provide both localized spin and hole. Up to now, there is no completely adequate model describing an origin of ferromagnetic ordering of spins in DMS. This question is still rather controversial. According to one of the most used the p-d Zener model, which can be applied to p-type DMS,⁴ the ferromagnetic ordering of localized spins occurs due to exchange interaction with holes. This model predicts an increase of Curie temperature with increasing Mn concentration. However, as it was shown, e.g., by Mack *et al.*,⁵ the increased Mn content did not raise Curie temperature. At present, the highest observed Curie temperature for (Ga,Mn)As thin films is about 180 K,⁶ which is still far from the room temperature. Usually the low temperature regime is used for the MBE growth (LT-MBE) of (Ga,Mn)As thin films, i.e., 200–350 °C, to avoid the segregation of secondary phases such as MnAs having hexagonal α -phase with a Curie temperature of about 330 K and metallic conductivity.⁷ At temperatures lower than 250 K, the formation of antisite defects (As_{Ga}) as well as interstitial Mn atoms acting as double donors can occur, resulting in lowering the hole concentration. To decrease the concentration of Mn interstitials the

post-growth annealing procedure can be applied.⁸ Despite the considerable progress in the study of DMS, many questions are still unclear. One of them concerns the fabrication and the behavior of the low-dimensional structures based on DMS materials, such as nanowires (NWs).

Such quasi-one-dimensional structures can exhibit unique properties even due to their geometrical shape, for instance, the orientation of their easy magnetic axis is along the growth direction. So the magnetic properties of the samples can be in principle predetermined. Recently, NWs based on (Ga,Mn)As DMS materials have been grown by MBE.^{9–12} It should be noted, that NWs are usually obtained by the so-called vapor–liquid–solid (VLS) mechanism on the substrates activated by a metal growth catalyst.^{13,14} The most commonly used catalytic metal is gold. On the other hand, the self-catalyzed NWs can be also obtained.¹⁵ Usually, the typical temperatures used for the MBE growth of GaAs NWs lie between 450 and 640 °C. But as it was mentioned above, this temperature window can lead to segregation of MnAs during the MBE growth of (Ga,Mn)As thin films. Therefore, one of the approaches to the growth of (Ga,Mn)As NWs is to use the lowered temperatures similar to the thin films. For example, the temperature range of 300–350 °C was used to synthesize (Ga,Mn)As with preliminary deposited MnAs nanoislands as a catalyst for the growth.⁹ The NWs obtained had many branches as well as MnAs nanoclusters and were tapered. Another two-stage method was also applied to form (Ga,Mn)As NWs at low temperatures.¹¹ First, a GaAs NW core was grown at 540 °C by Au-assisted MBE. Then, the substrate temperature was lowered to 200–300 °C and the (Ga,Mn)As shell was deposited. The shell was highly inhomogeneous. The Curie temperature of samples obtained was around 30 K. The method based on the use of Mn as a catalyst for the formation of GaAs NWs was shown by Martelli *et al.*¹⁶ A similar

^{a)}Author to whom correspondence should be addressed. Electronic mail: bour@mail.ioffe.ru.

approach was applied to the MBE growth of (Ga,Mn)As at elevated growth temperatures.¹² The NWs obtained on GaAs(111)B substrate surface at 660 °C exhibited paramagnetic behavior.¹² In this paper, we report on the study of structural, optical, and magnetic properties of (Ga,Mn)As NWs grown on GaAs(001) at intermediate temperatures higher than the ones used for LT-MBE growth of (Ga,Mn)As thin films, but a bit lower than the ordinary temperatures of Au-assisted MBE growth of GaAs NWs.

II. EXPERIMENTAL

The growth experiments were carried out using an EP1203 MBE system equipped with Ga, Mn atomic and As₄ molecular cells. First, epi-ready GaAs(001) substrates were thermally cleaned to eliminate native oxide overlayer at 620 °C. The deoxidation process was monitored by the reflection high-energy electron diffraction (RHEED) method. The temperatures of the cells were equal to 1000, 373, and 720 °C, correspondingly for Ga, As, and Mn. After completion of the oxide removing process, the temperature of the substrate was lowered by 40–50 °C, and the growth of the GaAs buffer layer was carried out over 15 min to smooth out the surface. Then the temperature was decreased by another 10 °C and Mn shutter was opened (As shutter was closed during Mn deposition stage) for 2 min to form nanoclusters used as a catalyst for the self-catalyzed growth of NWs. As the working temperature (485 °C) was reached, the Mn, Ga, and As cells were simultaneously opened, and the (Ga,Mn)As NWs immediately started to grow. The time of NW nucleation evaluated from RHEED pattern was 30 s. The total growth time was equal to 25 min at the GaAs growth rate equal to 1 ML/s. It should be noted, that the growth of NWs occurred under metal stabilized growth conditions. The As/(Ga,Mn) flux ratio was 0.4.

III. RESULTS AND DISCUSSION

The morphology of the NWs obtained was studied using a scanning electron microscope (SEM) Zeiss Supra 25. SEM images of (Ga,Mn)As NWs shown in Figure 1 demonstrate that NWs have typical lengths between 0.8 and 4 μm and diameters 50–90 nm. The nanowire density is about 10⁷ cm⁻². Most of NWs have a preferential growth direction along <111> and <110>. Some of them are oriented along <310>



FIG. 1. SEM images of plane view of (Ga,Mn)As NWs arrays.

crystallographic directions. In contrast,⁹ the (Ga,Mn)As NWs do not have any branches. Many of them are slightly tapered, which can be caused by the relatively low growth temperature resulting in limitations on Ga adatom diffusion lengths.^{17,18}

The structural and chemical characterization of the grown samples was carried out by transmission electron microscopy. For this purpose, the samples were prepared in two different ways. First, the NWs were chopped from the substrate and suspended on a carbon grid. The growth direction of the NWs and their morphology were analyzed in a Jeol JEM 4010 microscope, which allowed a high-resolution TEM investigation (HRTEM) of the crystal structure including lattice defects. Second, the chemical nature of precipitates found on the substrate surface as well as the chemical composition were investigated by high-angle angular dark-field scanning transmission electron microscopy (HAADF-STEM) combined with energy-dispersive X-ray analysis (EDX). For this analysis, we used a FEI TITAN 80/300 equipped with a probe corrector, which allowed a lateral resolution of 0.1 nm.

Figure 2 shows a typical example of a <110> oriented NW obtained as a result of TEM analysis. The NW has a length of 2 μm, thickness <100 nm, and it is slightly tapered. In such long NWs, we could not find crystal defects, such as dislocations or precipitates. However, some of them contain planar features as stacking faults lying parallel to the growth direction (see Figure 2). The NWs have a zincblende crystal structure. The EDX analysis of (Ga,Mn)As also yielded no local precipitation of the Mn within the detection limit of 0.5%. Thus, Mn can be homogeneously distributed in the NWs. However, some of them contain planar features such as stacking faults lying parallel to the growth direction (see Figure 2).

Despite the fact that the TEM investigation of (Ga,Mn)As NWs has not shown the presence of any

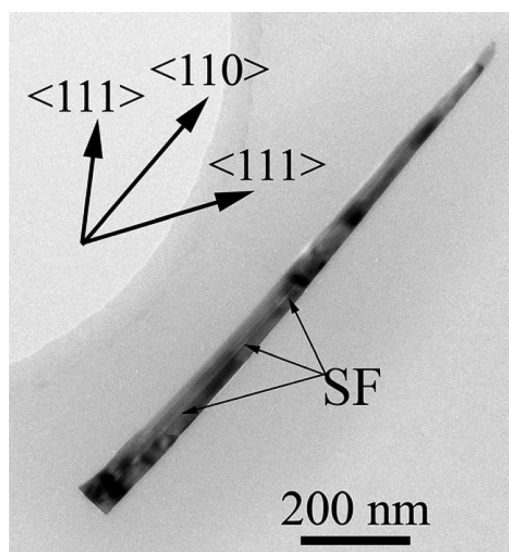


FIG. 2. TEM image of a <110> oriented NW. The tip at the upper right contains the growth front and the catalytic droplet, which contains a high concentration of Mn. The dark features inside the NWs are caused by bending of the crystal lattice, known as "bending contours." In the center, a stacking fault (SF) is located lying parallel to the growth direction.

precipitates on their side-walls as well as inside the NWs, surprisingly, precipitates were found between the NWs at the interface of the wetting layer (see Figure 3). As it can be seen, the precipitates with hemispheric shape have lateral sizes between 100 and 200 nm and depth about 50 nm. They have relatively high density with an average distance between them of about 1 μm . The chemical nature of precipitates found on the substrate surface as well as the chemical composition was investigated by HAADF-STEM combined with EDX. It was shown that Mn content inside precipitates is close to 50%, while Ga concentration seems to be very low mainly coming from the surrounding GaAs matrix. The diffractogram presented in the insert of Figure 3 indicates that the precipitate might have a hexagonal phase. Thus, it seems that during the MBE growth of (Ga,Mn)As NWs, a segregation of α -MnAs precipitates in hemispherical shape simultaneously occurred, having hexagonal crystal structure similar to NiAs-type.^{7,18,19}

The magnetic properties of the samples with (Ga,Mn)As NWs were measured using a superconducting quantum interference device (SQUID) magnetometer Quantum Design MPMS-XL7. The samples were placed in the center of the plastic tubes used as sample holders and fixed mechanically without any additional fixing material. The magnetic field was parallel to the sample surface. The measurements were performed in the sample vibrating mode (Reciprocating Sample Option). The temperature dependences of the magnetization demonstrate that the samples with (Ga,Mn)As exhibit ferromagnetic properties up to temperatures higher than room temperature (Figure 4(a)). Such a behavior seems to be caused by the presence of MnAs precipitates, which were found to be segregated during the growth of NWs, since they demonstrate similar dependences of magnetization.¹⁹ The Curie temperature of the samples is similar to a value obtained for MnAs clusters (~ 330 K). The shape of the zero-field-cooling (ZFC) curve indicates a progressive blocking

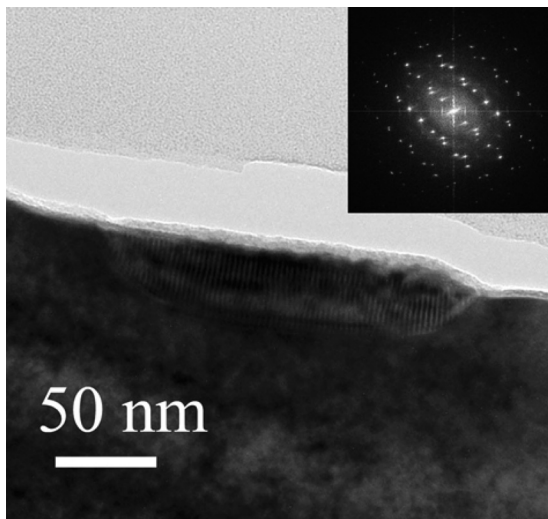


FIG. 3. TEM overview of a cross-section sample. It shows the precipitate near/at the surface of the grown GaAs layer by its Moiré-contrast. In the top right corner, the Fourier-transform of HREM image is inserted. It demonstrates the MnAs phase by the extra reflections in addition to the GaAs matrix reflections.

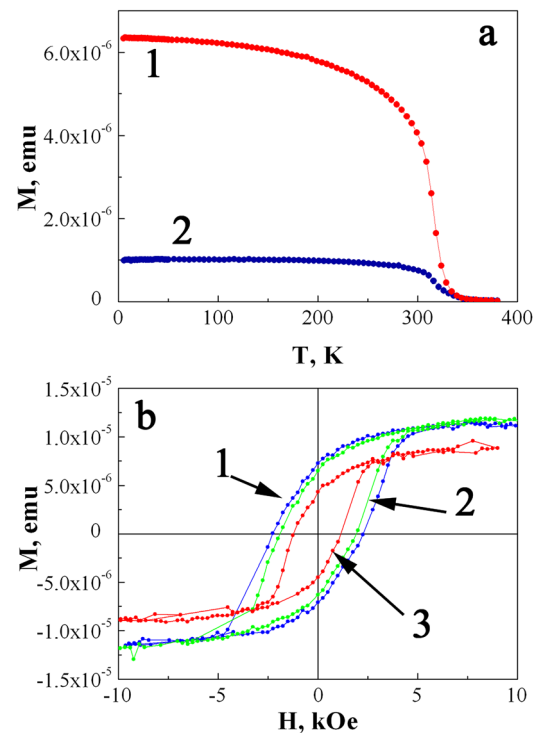


FIG. 4. (a) Temperature dependences of magnetization measured in an applied field of 100 Oe of the sample with (Ga,Mn)As NWs after field cooling (FC) (1) and zero-field cooling (ZFC) (2). (b) Magnetic field dependences of magnetization measured at: 10 K—(1), 200 K—(2), and 300 K—(3).

of the precipitate's moments in a wide temperature range (Figure 4(a)), probably due to the deviations of their sizes. The field dependences of magnetization of the samples are shown in Figure 4(b). They demonstrate the presence of clearly resolved hysteresis loops. The maximum value of a coercive field obtained at 10 K corresponds to 2250 Oe (Figure 4(b)). Thus, magnetic properties of the samples with (Ga,Mn)As seem to be conditioned by the formation of hexagonal α -MnAs nanoprecipitates.

In order to diminish an influence of MnAs precipitates formed between (Ga,Mn)As NWs, the NWs were peeled off from the substrate by the following procedure. First, the sample with NWs was cut into small pieces. Then, they were one by one immersed into ethanol and placed into ultrasonic bath for 2 min. The (Ga,Mn)As NWs were broken from the host GaAs(001) substrate and dispersed into solution. Afterwards, the solution with NWs was pipetted through the filter paper. Ethanol was evaporated, and NWs were left on the paper. The procedure was repeated several times, since the density of NWs was rather low. The temperature dependence of magnetization of the (Ga,Mn)As NWs obtained is shown in Figure 5. The measurements were performed in an applied magnetic field of 200 Oe, i.e., higher, than it was used for the samples with standing NWs, since the signal was considerably weaker due to the low quantity of NWs dispersed. The dependence exhibits ferromagnetic behavior up to ~ 70 K (see Figure 5). Galichka *et al.*²⁰ have shown using *ab initio* calculations that in zincblende (Ga,Mn)As NWs magnetic properties can be suppressed compared to wurtzite ones due to the distribution of Mn at the side facets. Possibly, this

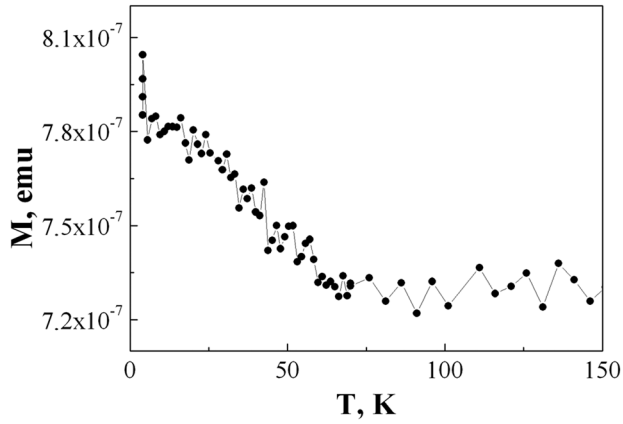


FIG. 5. Temperature dependences of magnetization measured in an applied field of 200 Oe of the (Ga,Mn)As NWs peeled off from the substrate.

relatively low Curie temperature can be explained by taking into account these similar reasons. However, we did not observe any noticeable Mn segregation on the NW sidewalls. Recently, Sadowski *et al.*²¹ have demonstrated that Mn-rich (Mn,Ga)As nanocrystals embedded in GaAs using additional temperature annealing of (Ga,Mn)As layers grown by MBE at 270 °C can exhibit ferromagnetic or superparamagnetic-like behavior. Despite the fact that we have not found by TEM any presence of such nanocrystals inside our NWs, the Mn–Ga droplets on the NW tips might have similar features.

Additionally, the investigation of magneto-optical properties of the samples with (Ga,Mn)As NWs by hot-electron photoluminescence (HPL) has been performed.^{22,23} The photoluminescence (PL) spectra of samples were measured using a He–Ne laser for excitation with a photon energy of 1.96 eV and Dilor XY800 spectrograph equipped with CCD matrix. The PL polarization in a magnetic field was studied using a photoelastic quartz modulator. Magnetic fields up to 5 T were generated by a superconducting magnet. The measurements were performed in Faraday geometry.

The PL spectra obtained are shown in Figure 6(a). The peak at about 1.517 eV can be connected to an exciton (X), whereas the line at 1.505 eV can be caused by the well known transition of a free electron to a neutral acceptor ($e-A_{\text{C}}^0$) in GaAs. The broad emission bands ($e-A_{\text{Mn}}^0$) around 1.411 eV and the corresponding TA-phonon and LO-phonon replica consisting of two series of lines and can be due to the recombination of the equilibrium photoexcited free electrons with holes bound to neutral Mn acceptors. Thus, Mn atoms substitute Ga sites in crystal lattice. We have compared the results obtained with the data of the PL investigation of 1000 nm (Ga,Mn)As layer (Mn atom concentration was about $5 \times 10^{17} \text{ cm}^{-3}$) taken from Ref. 23 and marked as R (reference sample) in Figure 6(a). It should be mentioned that R was grown by MBE on a GaAs(001) substrate at 560 °C and revealed paramagnetic behavior.²³ There is a small blue shift of about 3 meV of the $e-A_{\text{Mn}}^0$ PL band in the sample with NW as compared to that of R (Figure 6(a)). This shift seems to be caused by the confinement effects in NWs. Moreover, the full line half width (FLHW) is smaller in the case of the sample with NWs. The concentration of Mn of the NW sample can be estimated roughly as about 1×10^{18}

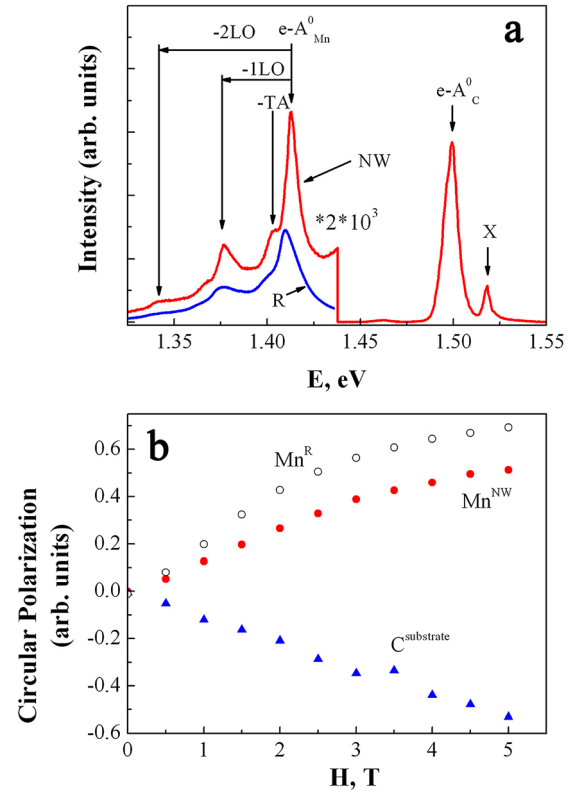


FIG. 6. (a) PL spectra of sample with (Ga,Mn)As NWs (NW) and reference one (R) excited with $\hbar\omega_{\text{ex}} = 1.96 \text{ eV}$ measured at 2 K. The recombination of equilibrium electrons with holes bound to Mn acceptor is marked by the arrow $e-A_{\text{Mn}}^0$. Peaks labeled as “1LO” and “2LO” are the first and second LO replica of the $e-A_{\text{Mn}}^0$ band. The lines $e-A_{\text{C}}^0$ and X are related to shallow acceptor (carbon) and exciton recombination in substrate; (b) PL polarization measured on Mn (solid circles) as well as C (solid triangles) acceptors in the sample with NWs and Mn (open circles) in reference (R) sample.

cm^{-3} from the intensity of the lines compared to R sample. Another important signature of Mn acceptor related PL is demonstrated in Figure 6(b), which represents the results of an investigation of PL polarization in an applied magnetic field. The antiferromagnetic exchange interaction between the $3d^5$ electrons of the inner Mn shell and bound valence band holes²³ leads to the sign reverse of PL (solid circles in Figure 6(b)) in comparison with the non magnetic acceptor (solid triangles in Figure 6(b)). Figure 6(b) also shows the data of the sample R. It seems that confinement in the NWs reduces the PL polarization.²⁴ It should be taken into account that we have studied the magneto-optical properties of the sample with (Ga,Mn)As NWs. As TEM investigation has shown, there was segregation of MnAs precipitates at the sample surface. Since they exhibit a metallic type of conductivity, they will not contribute to the PL. But, the surface layer between NWs can be unintentionally doped with Mn too. Therefore, we cannot exclude this possibility. In contrast to the SQUID data PL polarization of the NW sample shows rather paramagnetic behavior in an applied magnetic field (Figure 6(b)). This means that the density of Mn acceptors is not too high, resulting in weak coupling between neighboring Mn acceptors²⁴ or that the signal is obtained not only from (Ga,Mn)As NWs themselves, but also from the layer between them. In order to disjoint the contribution of

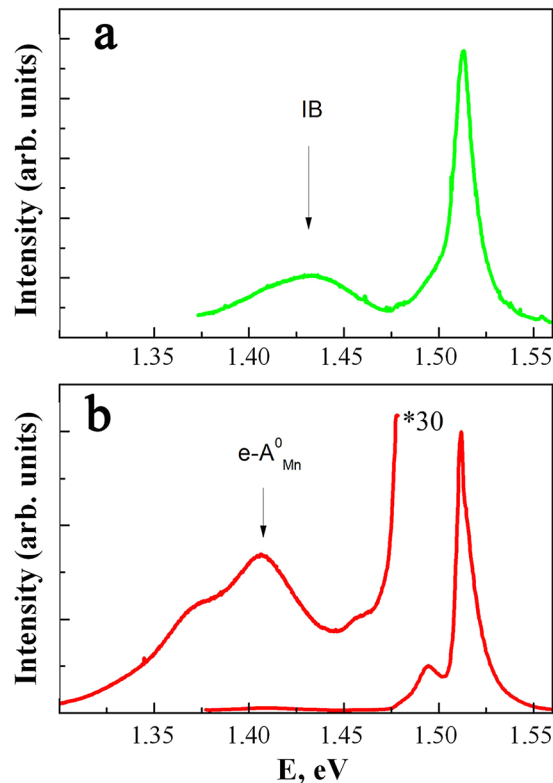


FIG. 7. PL spectra of (Ga,Mn)As NWs deposited onto Si substrate (a) compared to one of as grown sample with NWs (b) excited with $\hbar\omega_{ex} = 1.96$ eV measured at 77 K.

different parts, the NWs were peeled off from the host substrate and deposited onto a Si substrate using the procedure described above. Since the density of the NWs on the Si substrate was quite low, the experiments were carried out only at 77 K, because the constructive features of our PL setup do not allow for moving the sample inside the He cryostat. The results of measurements of peeled off nanowires as well as the sample with (Ga,Mn)As nanowires are shown in Figures 7(a) and 7(b), respectively. As it can be seen from the comparison of Figures 7(a) and 7(b), the line corresponding to the recombination of the equilibrium photoexcited free electrons with holes bound to neutral Mn acceptors became much broader and the position of its maximum shifted to the higher energies in case of peeled off NWs. Like in a case of DMS, such behavior can be due the formation of impurity band.²³ Thus, the results obtained are in a good agreement with the SQUID data for peeled off NWs despite the slight difference in the temperatures which can be induced by low level of detected SQUID signal due to small amount of NWs (see Figure 5).

IV. CONCLUSIONS

In summary, (Ga,Mn)As NWs have been grown by MBE on GaAs(100) substrates using Mn as a catalyst. The majority of the NWs have preferential growth direction along $\langle 111 \rangle$ and $\langle 110 \rangle$. The NWs do not have any extended defects, such as dislocations or precipitates. The EDX analysis of (Ga,Mn)As also yielded no local precipitation of Mn within

the detection limit of 0.5%. Some of the NWs contain planar features such as stacking faults lying parallel to the growth direction. It was found that during the MBE growth of (Ga,Mn)As NWs, the segregation of α -MnAs precipitates in a hemispherical shape occurred between the NWs near/at the surface of the grown GaAs layer. The magnetic properties of the samples with (Ga,Mn)As seem to be conditioned by the formation of α -MnAs precipitates. However, (Ga,Mn)As NWs themselves demonstrate ferromagnetic behavior up to ~ 70 K. PL measurements of the sample with (Ga,Mn)As NWs exhibit broad emission bands ($e-A_{Mn}^0$) around 1.411 eV and the corresponding TA-phonon and LO-phonon replica consisting of two series of lines, which can be caused by the recombination of the equilibrium photoexcited free electrons with holes bound to neutral Mn acceptors. The investigation of (Ga,Mn)As NWs peeled off from the substrate performed at higher temperatures has shown that the above-mentioned band at 1.411 eV became broader and the position of its maximum shifted to the higher energies. It can be caused by the formation of an impurity band. The results obtained are of importance for the realization of new spintronic devices based on DMS nanowires.

ACKNOWLEDGMENTS

We would like to thank Richard Stone for the constructive remarks. We acknowledge the financial support from the different programs of RAS, RFBR, FP7 EU projects and from different contracts with Russian Ministry of Education and Science.

- ¹T. Dietl, *Nature Mater.* **9**, 965–974 (2010).
- ²H. Ohno, *Science* **281**, 951–956 (1998).
- ³H. Ohno, *Nature Mater.* **9**, 952–954 (2010).
- ⁴T. Dietl, H. Ohno, F. Matsukura, J. Cibert, and D. Ferrand, *Science* **287**, 1019–1022 (2000).
- ⁵S. Mack, R. C. Myers, J. T. Heron, A. C. Gossard, and D. D. Awschalom, *Appl. Phys. Lett.* **92**, 192502 (2008).
- ⁶M. Wang, R. P. Campion, A. W. Rushforth, K. W. Edmonds, C. T. Foxon, and B. L. Gallagher, *Appl. Phys. Lett.* **93**, 132103 (2008).
- ⁷D. Kolovos-Vellianitis, C. Herrmann, L. Däweritz, and K. H. Ploog, *Appl. Phys. Lett.* **87**, 092505 (2005).
- ⁸K. W. Edmonds, P. Boguslawski, K. Y. Wang, R. P. Campion, S. N. Novikov, N. R. S. Farley, B. L. Gallagher, C. T. Foxon, M. Sawicki, T. Dietl, M. Buongiorno Nardelli, and J. Bernholc, *Phys. Rev. Lett.* **92**, 037201 (2004).
- ⁹J. Sadowski, P. Dłuzewski, S. Kret, E. Janik, E. Lusakowska, J. Kanski, A. Presz, F. Terki, S. Charar, and D. Tang, *Nano Lett.* **7**, 2724–2728 (2007).
- ¹⁰J. Sadowski, A. Siusys, A. Kovacs, T. Kasama, R. E. Dunin-Borkowski, T. Wojciechowski, A. Reszka, and B. Kowalski, *Phys. Status Solidi B* **248**, 1576–1580 (2011).
- ¹¹A. Rudolph, M. Soda, M. Kiessling, T. Wojtowicz, D. Schuh, W. Wegscheider, J. Zweck, C. Back, and E. Reiger, *Nano Lett.* **9**, 3860–3866 (2009).
- ¹²A. D. Bouravleuv, G. E. Cirlin, V. V. Romanov, N. T. Bagraev, E. S. Brilinskaya, N. A. Lebedeva, S. V. Novikov, H. Lipsanen, and V. G. Dubrovskii, *Semiconductors* **46**, 179–183 (2012).
- ¹³R. S. Wagner and W. C. Ellis, *Appl. Phys. Lett.* **4**, 89–90 (1964).
- ¹⁴E. I. Givargizov, *J. Cryst. Growth* **31**, 20–30 (1975).
- ¹⁵G. E. Cirlin, V. G. Dubrovskii, Yu. B. Samsonenko, A. D. Bouravleuv, K. Durose, Y. Y. Proskuryakov, B. Mendes, L. Bowen, M. A. Kaliteevski, R. A. Abram, and D. Zeze, *Phys. Rev. B* **82**, 035302 (2010).
- ¹⁶F. Martelli, S. Rubini, M. Piccin, G. Bais, F. Jabeen, S. De Franceschi, V. Grillo, E. Carlino, F. D'Acapito, F. Boscherini, S. Cabrini, M. Lazzarino, L. Businaro, F. Romanato, and A. Franciosi, *Nano Lett.* **6**, 2130–2134 (2006).

- ¹⁷V. G. Dubrovskii, N. V. Sibirev, G. E. Cirlin, M. Tchernycheva, J. C. Harmand, and V. M. Ustinov, *Phys. Rev. E* **77**, 031606 (2008).
- ¹⁸J. De Boeck, R. Oosterholt, A. Van Esch, H. Bender, C. Bruynseraede, C. Van Hoof, and G. Borghs, *Appl. Phys. Lett.* **68**, 2744–2746 (1996).
- ¹⁹M. Moreno, A. Trampert, L. Daeweritz, and K. H. Ploog, *Appl. Surf. Sci.* **234**, 16 (2004).
- ²⁰M. Galicka, R. Buczko, and P. Kacman, *Nano Lett.* **11**, 3319–3323 (2011).
- ²¹J. Sadowski, J. Z. Domagala, R. Mathieu, A. Kovacs, T. Kasama, R. E. Dunin-Borkowski, and T. Dietl, *Phys. Rev. B* **84**, 245306 (2011).
- ²²D. N. Mirlin, I. Ja. Karlik, L. P. Nikitin, I. I. Reshina, and V. F. Sapega, *Solid State Commun.* **37**, 757 (1981).
- ²³V. F. Sapega, M. Ramsteiner, O. Brandt, L. Däweritz, and K. H. Ploog, *Phys. Rev. B* **73**, 235208 (2006).
- ²⁴V. F. Sapega, O. Brandt, M. Ramsteiner, K. H. Ploog, I. E. Panaiotti, and N. S. Averkiev, *Phys. Rev. B* **75**, 113310 (2007).